

THE RECESSION OF THE DORSA ARGENTEA FORMATION ICE SHEET: GEOLOGIC EVIDENCE AND CLIMATE SIMULATIONS. K. E. Scanlon and J. W. Head, Brown University Department of Earth, Environmental and Planetary Sciences, Providence, RI 02912 USA. *kathleen_scanlon@brown.edu*

Introduction: The Dorsa Argentea Formation (DAF) covers $\sim 1.5 \times 10^6 \text{ km}^2$ surrounding and slightly offset from the south pole of Mars [1-3]. It is characterized by pitted terrains; branched, sinuous ridges; and plains units with lobate, rounded margins [1-3]. Topographic, image, radar, and spectral data have supported the interpretation [3] that the DAF is the remnant of a large Noachian-Hesperian ice sheet where abundant melting occurred. Specifically: (a) sinuous ridges within the deposit are interpreted as eskers [3, 4] on the basis of their scale, spacing, cross-sectional shape, sinuosity, branching patterns, branching angles, relationship to underlying topography, and stratigraphic location consistent with subglacial formation [3, 5, 6]; (b) fluvial channels hundreds of kilometers long head in the DAF and breach impact craters to create open-basin lake systems on both sides of the 0° lobe [7, 8]; features in Argentea Planum are also consistent with a large paleolake in that region [9]; (c) the steep-sided, flat-topped Sisyphi Montes have been interpreted as subglacially erupted volcanoes on the basis of their morphology, morphometry, and distribution [10]; this interpretation has been bolstered by the enhanced concentrations of hydrated sulfates in the edifices themselves [11, 12]; (d) radar reflectors with the same footprint as the DAF are consistent with present-day volatiles in the deposit [13].

In recent years, better image coverage and higher image resolution in the DAF region have become available, allowing further evaluation of these geomorphological interpretations. Furthermore, Global Climate Models have been developed that allow simulations of possible Late Noachian – Early Hesperian climate conditions on Mars. We revisit the interpreted fluvial features in the DAF with higher-resolution data. We also use a suite of Early Mars climate simulations with the LMD Generic Climate Model [14, 15] to interpret the distribution of glaciofluvial landforms and the age and preservation of esker populations within the DAF in the context of climate change at the Noachian-Hesperian boundary.

Fluid flow properties in subglacial tunnels: The observation [3, 5, 6] that eskers within the DAF ascend topographic slopes indicates that the corresponding subglacial channels below the DAF ice sheet were filled completely by water, such that flow was driven by hydraulic pressure rather than gravity. Fluxes through these tunnels and the slope of the overlying ice can therefore be calculated from esker morphometry and distribution.

Fluxes. Banks et al. [16] used a simplified form of the Darcy-Weisbach equation to estimate the fluxes recorded by eskers in Argyre basin. Following their meth-

ods, assuming a triangular channel cross-section with a flow depth of 1 or 10 m and a medium sand or coarse gravel channel bed, and measuring channel width and bottom slope in large, single-crested eskers among the Dorsa Argentea, we estimate fluvial discharge on the order of $1 \cdot 10^3 - 1 \cdot 10^5 \text{ m}^3 \text{ s}^{-1}$. These are comparable to the values derived for the Argyre eskers [16], as might be expected if both developed under similar climate conditions. For comparison, typical summer discharges from beneath the 40 km long Kennicott Glacier in Alaska are of the order $\sim 10^2 \text{ m}^3 \text{ s}^{-1}$ [17], but flood discharges of the order $10^6 \text{ m}^3 \text{ s}^{-1}$ have occurred beneath Arctic and Antarctic ice sheets in the past [e.g. 18, 19]. We are using the values and spatial distribution of fluxes measured from DAF eskers with GCM simulations to constrain the climate under which the DAF ice sheet receded.

Ice surface slope. Under channel-full conditions, the vector sum of the topographic gradient along an esker, the regional dip (multiplied by a constant), and the slope of the ice surface at the time of esker formation is zero [20]. To calculate ice slope from present-day topography and esker paths, we sought well-preserved eskers in regions whose topography is not obscured by glacial debris. Ice slopes calculated over Dorsa Argentea esker systems fitting these criteria are small, of the order 0.1 m km^{-1} throughout. This implies that these eskers formed in a thick, flat, interior region of the ice sheet rather than near its edge, where slopes are expected to be steeper. This scenario is consistent with other evidence [3] for many eskers in the DAF having formed by basal melting, controlled partially by the thickness of the overlying ice. It is also consistent with the comparatively young exposure age of this esker population [21], which suggests that it remained ice-covered longer than populations in other parts of the DAF. Eskers in the Argyre basin appear to have formed closer to the glacier edge, allowing Bernhardt et al. [22] to constrain the thickness ($\sim 2 \text{ km}$) of the Argyre paleo ice sheet from calculated ice slopes. Analysis of other esker populations within the DAF is ongoing and may allow the DAF paleo ice sheet thickness to be determined in those regions.

New images of previously described glaciofluvial features: New images bolster previous interpretations of glaciofluvial landforms within the DAF. For example, several of the channels heading in the DAF breach impact craters downstream, creating open-basin lake systems. Ghatan and Head [8] noted fan-shaped deposits at the mouth of the upstream channel in several of these crater lakes. HiRISE images reveal horizontal layering in these deposits, consistent with a sedimentary origin. Ad-

ditionally, several esker systems terminate in the region interpreted by [9] as a proglacial lake. CTX images reveal that some of these appear to terminate in layered fan-shaped deposits, typical of eskers terminating in standing water [e.g. 23].

Global Climate Model simulations: The size and density of eskers in the DAF indicates that substantial melting occurred during their construction. The large size of DAF eskers is easier to explain by terrestrial standards if a component of the flow through them derived from melting at the glacier surface, propagated downward to subglacial channels through vertical ice fractures. The excellent preservation of many eskers, however, is more consistent with a bottom-up melting mechanism, where the thickness of the ice sheet allowed ice to melt at its base despite below-freezing surface temperatures. In a bottom-up melting scenario, after the ice had thinned to the point where basal melting could no longer occur, the cold-based ice would preserve the underlying landforms [21], whereas top-down melting would have continued regardless of ice thickness.

Conditions for surface and basal melting. We first assess the likelihood of basal melting by conducting a GCM climate simulation with a 1 bar CO₂ atmosphere and 25° spin-axis obliquity. Fastook et al. [24] calculated that, for ice thickness ~2 km (consistent with minimum estimates from tuya heights, [10]), annual average temperatures between -75°C (if late Noachian geothermal fluxes were 65 mW m⁻²) and -50°C (for 45 mW m⁻²) would allow basal melting to occur. Annual average temperatures in the 1 bar, 25° obliquity climate scenario are between -57 and -59°C in the regions of the DAF where eskers are densest. Basal melting could therefore have occurred even at low obliquity and in a cold early martian climate, for all but the most conservative geothermal flux. We are currently conducting GCM simulations with higher spin-axis obliquity, as well as a “warm, wet, early Mars” end-member climate scenario with annual average temperatures above freezing, in order to constrain the climate conditions under which top-down melting could have occurred, as well as those under which the rate and spatial pattern of ice removal could be consistent with geological observations.

Relationship to age of esker populations. Kress and Head [21] used buffered crater counting to determine exposure ages for five esker populations within the DAF. The youngest populations, i.e. those whose overlying ice was most recently removed, lie along the 90°W lobe of the DAF. Populations on the other side of the DAF are several hundred million years younger. While glacial flow modeling will be necessary to fully describe the topography of the DAF ice sheet under plausible paleoclimate conditions, the coldest annual average temperatures at the south pole in our baseline climate scenario

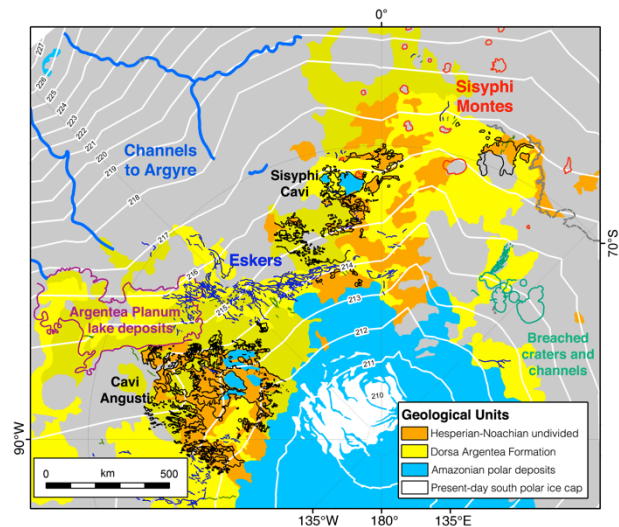


Figure 1. The Dorsa Argentea Formation. Geologic units shown as mapped by [2]. White, labeled contours are annual average GCM temperatures (°K). Eskers mapped in dark blue.

extend along the 90°W lobe (Figure 1). This could have allowed particularly effective ice preservation in this part of the deposit. The annual average temperature pattern also shows a lobe extending along the 0°W meridian, suggesting that the asymmetry of the DAF may reflect asymmetry in the former ice sheet.

Conclusions: Our morphometric analysis of the Dorsa Argentea population of eskers within the DAF suggests that flow through the subglacial channels of the DAF ice sheet was of the order $10^3 - 10^5 \text{ m}^3 \text{ s}^{-1}$, and flat calculated ice sheet topography supports the hypothesis that these eskers formed due to bottom-up melting in a thick ice sheet and a cold martian climate. GCM simulations indicate that annual average temperatures could have supported basal melting in the DAF even for the 1 bar CO₂, 25° obliquity scenario. The temperature distribution at the south pole shows cold lobes extending along the 0° and 90°W meridians, which would have favored the development of asymmetric polar deposits recorded by the DAF and a thicker ice cover over the regions where the most abundant eskers are observed.

References: [1] Tanaka K. L. and Kolb E. J. (2001) *Icarus*, 154, 3–21. [2] Tanaka K. L. and Scott D. H. (1987) *USGS Misc. Invest. Ser. Map*, I-1802-C. [3] Head J. W. and Pratt S. F. (2001) *JGR*, 106, 12275–12299. [4] Howard A.D. (1981) *NASA TM 84211*, 286–288. [5] Head J. W. and Hallet B. (2001) *LPSC XXXII*, abstract #1366. [6] Head J. W. and Hallet B. (2001) *LPSC XXXII*, abstract #1373. [7] Milkovich S. M. et al. (2002) *JGR*, 107. [8] Ghatan G. J. and Head J. W. (2004) *JGR*, 109. [9] Dickson J. L. and Head J. W. (2006) *PSS*, 54, 251–272. [10] Ghatan G. J. and Head J. W. (2002) *JGR*, 107. [11] Wray J. J. et al. (2009) *Geology*, 37, 1043–1046. [12] Ackiss S. E. and Wray J. J. (2014) *Icarus*, 243, 311–324. [13] Plaut J. J. et al. (2007) *LPSC XXXVIII*, abstract #2144. [14] Wordsworth R. et al. (2013) *Icarus*, 222, 1–19. [15] Forget F. et al. (2013) *Icarus*, 222, 81–99. [16] Banks M. E. et al. (2009) *JGR*, 114, E09003. [17] Anderson S. P. et al. (2003) *Chem. Geol.*, 202, 297–312. [18] Shaw J. (1989) *Geology*, 17, 853–856. [19] Lewis A. R. et al. (2006) *Geology*, 34, 513–516. [20] Shreve R. L. (1985) *Quaternary Res.*, 23, 27–37. [21] Kress, A.K., and J. W. Head (2014) *PSS*, in press. [22] Bernhardt H. et al. (2013) *PSS*, 85, 261–278. [23] Brennand T. A. (2000) *Geomorphology*, 32, 263–293. [24] Fastook J.L. et al. (2012) *Icarus*, 219, 25–40.